

N O T I C E

THIS DOCUMENT HAS BEEN REPRODUCED FROM
MICROFICHE. ALTHOUGH IT IS RECOGNIZED THAT
CERTAIN PORTIONS ARE ILLEGIBLE, IT IS BEING RELEASED
IN THE INTEREST OF MAKING AVAILABLE AS MUCH
INFORMATION AS POSSIBLE

NASA Technical Memorandum 81391

RADIATION DAMAGE IN
LITHIUM-COUNTERDOPED
N/P SILICON SOLAR CELLS

A. M. Hermann
Tulane University
New Orleans, Louisiana

and

C. K. Swartz, H. W. Brandhorst, Jr., and I. Weinberg
Lewis Research Center
Cleveland, Ohio

Prepared for the
Fourteenth Photovoltaic Specialists Conference
sponsored by the Institute of Electrical and Electronics Engineers
San Diego, California, January 7-10, 1980

(NASA-TM-81391) RADIATION DAMAGE IN
LITHIUM-COUNTERDOPED N/P SILICON SOLAR CELLS
(NASA) 13 p HC A02/MF A01 CSCL 10A

N80-15557

Unclas
G3/44 46637

RADIATION DAMAGE IN LITHIUM-COUNTERDOPED N/P SILICON SOLAR CELLS

by A. M. Hermann*
Tulane University
New Orleans, Louisiana

and

C. K. Swartz, H. W. Brandhorst, Jr., and I. Weinberg
National Aeronautics and Space Administration
Lewis Research Center
Cleveland, Ohio

E-301

ABSTRACT

Lithium-counter-doped n⁺/p silicon solar cells were irradiated with 1 MeV electrons and their post-irradiation performance and low temperature annealing properties were compared to that of the 0.35 ohm-cm control cells. Cells fabricated from float zone and Czochralski grown silicon were investigated. It was found that the float zone cells exhibited superior radiation resistance compared to the control cells, while no improvement was noted for the Czochralski grown cells.

Room temperature and 60° C annealing studies were conducted. The annealing was found to be a combination of first- and second-order kinetics for short times. The defect migration energy found from the kinetic studies suggests that the principal annealing mechanism is migration of lithium to a radiation induced defect with subsequent neutralization of the defect by combination with lithium.

The effects of base lithium gradient were investigated. It was found that cells with negative base lithium gradients exhibited poor radiation resistance and performance compared to those with positive or no lithium gradients, the latter being preferred for overall performance and radiation resistance.

INTRODUCTION

In the past, extensive work has been carried out on the radiation resistance and annealing properties of p⁺/n silicon solar cells in which lithium is diffused into the n-type base (1,2). In general, it was found that the lithium-doped p⁺/n cells annealed at relatively low temperatures and were more radiation resistant to proton and neutron bombardment when compared to conventional n⁺/p silicon solar cells (3). At best, Li doped cells exhibited the same tolerance to 1 MeV electrons as the n⁺/p cells. Although for cells without lithium, it is known that the n⁺/p configuration exhibits superior radiation resistance, practically nothing is known concerning the effects of lithium counter-doping into the p-region of this configuration (4). Because lithium acts as a donor in silicon,

addition of lithium into boron-doped silicon is expected to result in increased resistivity through compensation. The impact of this increased resistivity on n⁺/p cell performance has not been studied. In view of the beneficial properties of lithium it is hoped that such counter-doping of the n⁺/p configuration will eventually lead to superior radiation resistance and post-irradiation annealing properties. In the present paper, we present the results of a preliminary, systematic investigation of radiation damage and annealing in lithium counter-doped n⁺/p cells. It is expected that the results of this investigation will lead to potentially fruitful pathways for future investigations of lithium-counter-doped silicon solar cells.

EXPERIMENTAL

Descriptions of the cells are given in Table I (5). Cells used in this study were nominally 300 μm thick, 2x2 cm, phosphorus diffused, n⁺/p silicon solar cells. Substrates were 0.35 ohm-cm, boron-doped, p-type Czochralski (CZ) and float zone (FZ) silicon. Lithium counter-doping was accomplished by applying a lithium paste (lithium dispersed in ether) to the cell back surface, and heating in nitrogen for 1/2 hour. In order to achieve different gradients, different amounts of lithium was applied to the back surface and drive-in temperatures were varied in the range of 450° to 500° C. The base lithium gradients listed in Table I were determined by four-point probe resistivity measurements at the cell back surface and C-V measurements at the cell junction to determine lithium concentrations. Lithium concentrations were determined from the difference between the known base doping concentration and the measured electrically active doping. The lithium gradients G_{Li} were then calculated from the relation:

$$G_{Li} = \frac{[Li]_B - [Li]_F}{t} \quad (1)$$

where [Li]_B and [Li]_F are lithium concentrations at the back surface and the junction, respectively, while t is cell thickness.

Pre-irradiation Air Mass Zero (AMO) solar cell parameters are listed in Table II. The Czochralski cells fabricated especially for this investigation

*NASA - American Society for Engineering Education Faculty Fellow.

did not include an antireflection (AR) coating. However, the float zone cells were off-the-shelf cells which included an AR coating. This accounts for the difference in solar cell AMO parameters (primarily current) in Table II. However, this difference in cells will not affect comparative factors such as short-circuit current ratios determined after irradiation. The reduced fill factor of the Czochralski cells was caused by insufficient metallization and does not affect any of the conclusions in this paper. AMO current-voltage characteristics were determined with a xenon-arc solar simulator, while spectral response was determined with a filter wheel apparatus (6). Diffusion lengths were measured using an X-ray excitation technique (7). The cells were irradiated by 1 MeV electrons to fluence as high as $10^{15}/\text{cm}^2$. Because the cells anneal at room temperature, they were stored in liquid nitrogen immediately after irradiation and were warmed to room temperature just prior to measurement. The cells were also annealed in air at room temperature and at 60°C .

EXPERIMENTAL RESULTS

A correlation between base lithium gradient and performance under irradiation is seen in Fig. 1. In general, cells with negative gradients perform poorly while the best performance is obtained for cells with either positive or zero lithium gradient. Thus, such gradients appear preferable to negative gradients.

The difference in spectral response between a negative gradient cell and a zero gradient cell is shown in Fig. 2. There was no significant difference in spectral response between the zero gradient and the control float zone cells. It can be seen that the negative lithium gradient reduces the spectral response at nearly all wavelengths except near $1.0\ \mu\text{m}$. The adverse effect of the negative lithium gradient can also be seen in the change of spectral response at short and long wavelengths with irradiation as demonstrated in Figs. 3 and 4. Cells with positive or zero gradients behave normally in the sense that principally the long wavelength response is affected by the irradiation. On the other hand, for cells with negative gradients (excess lithium near the junction), both long and short wavelength responses show substantial decreases.

Diffusion length damage coefficients K_L , are shown in Table III. The damage coefficients are obtained from the relationship:

$$\frac{1}{L^2} = \frac{1}{L_0^2} + K_L \phi \quad (2)$$

where L is diffusion length at fluence, L_0 is pre-irradiation value of the diffusion length, and ϕ is fluence of 1 MeV electrons. The K_L values cited are virtually identical to those expected for 0.35 ohm-cm boron-doped silicon. Thus, lithium counterdoping has no drastic effect on K_L . The slight increase in damage coefficient for Czochralski silicon compared to float zone is expected.

In general, lithium counterdoping improves the radiation resistance of cells fabricated from vacuum float zone grown silicon. Figure 5 shows the counterdoped float zone cell to have slightly better radiation tolerance than the control cell. Although the improvement is small, it must be stressed that no attempts at optimization were made in the present work. On the other hand, lithium-counter-doped cells fabricated from Czochralski silicon, showed no improvement over the control cells in the same test.

The results of annealing at room temperature and 60°C are shown in Figs. 6 to 9. For the room temperature annealing, the greatest diffusion length recovery occurs for cell 10 CZ (Fig. 6). However, the extent of the short-circuit current recovery for this negative lithium gradient cell (Fig. 7) does not correlate with the diffusion length recovery. In fact, none of the negative gradient cells show significant recovery of cell performance. Spectral response measurements confirm a slight increase in the $1.0\ \mu\text{m}$ response which correlates with the diffusion length measurement. However, there is no significant increase in response at other wavelengths, which predicts only a small recovery of current. We shall return to possible reasons for this anomaly in the discussion section. In general, however, both current and diffusion length recovery after room temperature annealing is significantly greater for the counter-doped cells than for the control cells. For the cells annealed at 60°C , it is recalled that the 1 MeV electron fluence in this case was $10^{15}/\text{cm}^2$, which makes annealing more difficult than is the case for those cells annealed at room temperature ($\phi = 3 \times 10^{14}/\text{cm}^2$). However, from Figs. 8 and 9 significant diffusion length and short-circuit current recovery occurs for the float zone cell while the counterdoped Czochralski cell shows insignificant recovery compared to the control cell.

DISCUSSION

The most significant aspects of post-irradiation cell behavior are cell performance and annealing, especially at the low temperatures used in this study. We treat each of these separately in the discussion which follows.

Cell Performance After Irradiation

The critical dependence of cell performance on base lithium gradient is well illustrated by the spectral response data of Figs. 3 and 4. Negative lithium gradients imply higher concentrations of lithium at the junction than at the back surface. One would expect that the presence of excess positive lithium ions near the junction would set up a drift field such that the passage of minority carriers to the junction would be facilitated. Existence of such a field can be inferred from diffusion length measurements in these cells. The negative gradient cells all have the longest diffusion lengths, even though processed from the same starting material. However, the short-circuit current of these cells does not show the effect of longer diffusion lengths. The loss in response is due to a general decrease in response below $0.95\ \mu\text{m}$.

The reason for this poor performance is open to speculation. From analysis of Fig. 2, it appears that the negative gradient cell has about 50% of the response of the undoped or zero gradient cells at wavelengths below about 0.7 μm . At longer wavelengths the percentage decrease gradually diminishes to zero. Light of 0.7 μm wavelength is absorbed (99.9%) within 20 μm depth in silicon. Therefore, it is postulated that the high concentrated ($\sim 4 \times 10^{16} \text{ cm}^{-3}$) of lithium in the first 10 to 20 μm of the cell either combines with an already-present defect to form a center which limits carrier lifetime or, of itself, causes lifetime degradation. Irradiation with 1 MeV electrons subsequently produces additional lifetime-reducing centers that create a narrow region near the junction with poor minority carrier lifetime. This effect is reminiscent of low energy proton damage in silicon solar cells. This recombination volume then limits cell current even though base diffusion length in the undamaged region may be long. In addition to defect formation, electron trapping effects may also act to limit cell performance.

Although negative gradient cells (5 FZ, 7 FZ, and 10 CZ) have the same lithium concentration near the junction, cell 10 CZ does not show a marked decrease in spectral response. It is speculated that the additional oxygen believed present in this cell may reduce the concentration of harmful defects prior to irradiation. After irradiation, all negative gradient cells behave the same.

The positive or zero gradient cells have lithium concentrations of about $1.7 \times 10^{16} \text{ cm}^{-3}$ near the junction. This reduction in lithium concentration compared to the negative gradient cells may be sufficient to prevent the formation of lifetime reducing centers before or after irradiation. We emphasize, however, the speculative nature of the phenomena invoked to explain the poor performance of cells with negative lithium gradients. Our results do, however, clearly indicate that positive gradients are preferably to negative base lithium gradients and that zero gradients appear to be the most desirable.

In addition, we have shown in a limited way, that lithium counterdoping improves the radiation resistance of n^+/p silicon solar cells to 1 MeV electron irradiation. Lithium-doped float zone cells were more resistant to radiation than the FZ control cells, whereas no such relationship was seen for cells made from Czochralski silicon. The superior performance of float zone over Czochralski silicon may be due to the reduced oxygen content of the float zone silicon. Optimization of all these factors, especially gradient and base lithium concentration is expected to lead to increased radiation resistance for lithium-counterdoped cells.

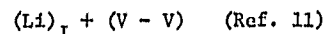
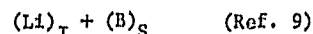
Annealing Behavior

Low Temperature Annealing: Low temperature annealing is desirable for extending the lifetime of cells in space and has been noted before in both lithium-counterdoped and p^+/n lithium-doped cells (4). The present counterdoped cells show superior

annealing characteristics over the control cells without any attempt at process optimization.

Examination of Figs. 6 and 7 reveals some apparently anomalous behavior. For example, cell 10 CZ exhibits the best diffusion length and extent of recovery. However, compared to 11 CZ which shows poor diffusion length recovery, the short-circuit current of 10 CZ is lower and its percent recovery in current is approximately the same. It is noted that 10 CZ has a negative lithium gradient while that for 11 CZ is positive. The diffusion length measurement principally yields the base diffusion length (7). Because cell current is controlled by phenomena occurring in both the base and near front surface region as discussed previously, there may not be a one-to-one correspondence between diffusion length and short-circuit current recovery. In general, it can be seen that cells with negative gradient usually show much better diffusion length recovery than short-circuit current recovery. The reason for this is not known.

Defect Structures and Annealing Kinetics: The purpose of examining annealing kinetics is to obtain insight into the annealing mechanism or mechanisms in this material. Although much is known concerning the defect structure when lithium is used as a donor in n-type silicon (8) almost nothing is known concerning the defects formed with lithium in p-type silicon. Knowledge of the possible defects is desirable before investigating the annealing kinetics in lithium-counterdoped silicon. A search of the literature disclosed the following defects identified as containing lithium in p-type silicon:



where the subscript I designates an interstitial and S a substitutional complex. Hence, there is evidence that lithium in p-type silicon forms additional defects with already existing defects. Annealing occurs when defects are neutralized by combination with lithium.

Additional information about the annealing process can be gained by studying the annealing kinetics. If the kinetics are first order, interactions occur principally between close pairs, and the following relationship holds (12):

$$N_D(t) = N_D(0) \exp - kt \quad (3)$$

where $N_D(t)$ and $N_D(0)$ are the defect concentrations at times t and zero, respectively, and k is the reaction rate constant. If E_m is the energy barrier for migration of lithium to the defect, then:

$$k = k_0 \exp(-E_m/k_B t) \quad (4)$$

where k_0 is the vibrational frequency of the defect in silicon and k_B is Boltzmann's constant. On the other hand, if the kinetics are second order, interactions occur principally between distant pairs, hence (12):

$$\frac{N_D(0)}{N_D(t)} = 1 + N_D(0)kt \quad (5)$$

It is customary to use diffusion length measurements in determining the type of kinetics. It is assumed that the radiative process creates one dominant defect from which it follows that (13):

$$\frac{1}{L^2} - \frac{1}{L_0^2} \propto N_D(t) \quad (6)$$

A plot of Eq. (3) (first-order kinetics) for room temperature annealing data is shown in Fig. 10. A similar plot has been made for the second-order kinetics using Eq. (5). Neither first- nor second-order kinetics prevails over the entire time range. However, for relatively short times, as shown in Figs. 11(a) and (b), the data give an equally good fit to either first- or second-order kinetics. The kinetics do not appear to depend upon the sign of the gradient. Similar results are obtained for the 60° C anneal.

Rate constants obtained from the first-order plots and Eq. (3) are shown in Table IV. Using Eq. (4), the defect migration energy is found to be $E_m \sim 0.8$ eV. Considering that data are available at only two temperatures and that the kinetics are not predominantly first or second order, the preceding value for E_m is considered approximate. However, the calculated value for E_m can be compared to the value of 0.66 eV (~ 0.7 eV) determined for the migration of lithium in silicon.

We conclude from the preceding discussion that a plausible mechanism for the annealing process is the migration of lithium to defects which are then neutralized by combination with the lithium. Although the defect structures listed previously form a base for study, it is premature to speculate further on the precise nature of the complexes formed between lithium and the irradiation-induced defects in boron-doped silicon that result in annealing.

CONCLUSIONS

Our preliminary survey of radiation resistance of lithium counterdoped cells is encouraging inasmuch as we find that lithium counterdoping improves the radiation resistance of n⁺/p silicon solar cells to 1 MeV electron irradiation. Additional conclusions obtained from the current work are:

Cells with zero or positive base lithium gradients exhibit superior radiation resistance and performance compared to cells with negative base lithium gradient.

Cells with zero lithium gradients exhibit the best radiation resistance.

Zero or positive gradient cells show partial annealing and recovery of performance at 25° and 60° C.

Annealing kinetics lie between first and second order for relatively short times.

The most likely annealing mechanism is diffusion of lithium to defects and subsequent neutralization of defects by combination with lithium.

These results indicate that additional work aimed at optimizing annealing and radiation resistance of the lithium counterdoped cells is warranted.

REFERENCES

1. P. A. Berman, "Effects of Lithium Doping on the Behavior of Silicon and Silicon Solar Cells," JPL Technical Report #32-1514, 1971. (NASA CR-116793)
2. P. A. Iles, "Lithium Solar Cell Technology," in Photovoltaic Specialists Conference, 9th., Silver Springs, Md., May 2-4, 1972, Record, New York: IEEE, 1972, pp. 296-302.
3. H. Y. Tada and J. R., Jr., Carter, "Solar Cell Radiation Handbook," JPL Publication 77-56, pp. 3-52, 1977. (NASA CR-155554)
4. R. G. Downing and J. R. Carter, "Study and Determination of an Optimum Design for Space Utilized Lithium Doped Solar Cells, Part II," TRW-13154-6022-RO-00, TRW Systems Group, Redondo Beach, Calif., 1971. (NASA CR-122942)
5. The cells used in this study were fabricated by Peter Iles at Applied Solar Energy Corp.
6. J. Mandelkorn, J. D. Broder, and R. P. Ulman, "Filter Wheel Solar Simulator," NASA TN D-2562, 1965.
7. W. Rosenzweig, "Diffusion Length Measurements by Means of Ionizing Radiation," Bell Syst. Tech. J., vol. 41, pp. 1573-1588, 1962.
8. J. M. Weingart, "Defect Structure and Behavior in Electron Irradiated, Lithium Diffused Silicon," in Photovoltaic Specialists Conference, 9th., Silver Springs, Md., May 2-4, 1972, Record, New York: IEEE, 1972, pp. 267-275.
9. R. C. Newman, Infra-Red Studies of Crystal Defects, New York: Barnes and Noble, 1973.
10. E. M. Pell, "Study of Li-O Interaction in Si by Ion Drift," J. Appl. Phys., vol. 32, pp. 1048, 1961.
11. R. C. Young, J. W. Westhead, and J. C. Corelli, "Interaction of Li and O with Radiation Produced Defects in Si," J. Appl. Phys., vol. 40, pp. 271-278, 1969.

12. J. W. Corbett, Electron Radiation Damage in Semiconductors and Metals, New York: Academic Press, 1966, pp. 36-43.
13. Shockley, W.; and Read, W. T., Jr., Statistics of the Recombination of Holes and Electrons. Phys. Rev., 87, 835, 1952.
14. Pell, E. M.: Diffusion Rate of Li in Si at Low Temperatures, Phys. Rev., 119, 1222, 1960.

TABLE I. - CELL DESCRIPTIONS

Cell no.	Base* resistivity, ohm, cm	Base lithium gradient, cm^{-4}	Description
1FZ	0.35	-----	Boron doped FZ control
2FZ	0.35	-----	Boron doped FZ control
3FZ	0.6	0	Lithium counterdoped FZ
4FZ	0.6	0	Lithium counterdoped FZ
5FZ	4	-8.7×10^{16}	Lithium counterdoped FZ
6FZ	4	-9.6×10^{16}	Lithium counterdoped FZ
7CZ	0.35	-----	Boron doped CZ control
8CZ	0.35	-----	Boron doped CZ control
9CZ	1.2	5.5×10^{17}	Lithium counterdoped CZ
10CZ	2	-2.3×10^{17}	Lithium counterdoped CZ
11CZ	2	9.1×10^{17}	Lithium counterdoped CZ

*Resistivity measured by four point probe at back surface after lithium doping (original base resistivity - 0.35 ohm-cm).

TABLE II. - INITIAL CELL PARAMETERS

Cell no.	I_{sc} , ma	V_{oc} , mV	P_{max} , mW	FF, %	Diffusion length, (μm)
1FZ	149.3	613	63.9	69.8	177
2FZ	147.5	621	70.9	77.4	185
3FZ	150.8	608	69.3	75.6	183
4FZ	148.3	592	56.3	64.1	163
5FZ	88.9	568	35.7	70.8	202
6FZ	92.1	569	37.1	70.8	203
7CZ	82.8	567	23.1	49.2	88
8CZ	84.6	556	22.3	47.4	77
9CZ	95.4	571	29.1	53.4	153
10CZ	89.8	568	29.0	56.8	199
11CZ	70.8	543	16.6	43.1	183

TABLE III. - DIFFUSION LENGTH

DAMAGE COEFFICIENTS

Cell no.	Damage coefficients, (K_L)
2FZ	3.2×10^{-10}
4FZ	3.4×10^{-10}
7CZ	4.7×10^{-10}
9CZ	3.4×10^{-10}

TABLE IV. - REACTION RATE CONSTANTS AND MIGRATION ENERGIES DETERMINED

USING FIRST ORDER KINETICS

Cell no.	Room temperature anneal					60° C anneal
	3FZ	5FZ	6FZ	10CZ	11CZ	4FZ
Rate constant - sec^{-1}	1.1×10^{-6}	1.1×10^{-6}	10^{-6}	1.3×10^{-6}	3.1×10^{-7}	2.9×10^{-5}

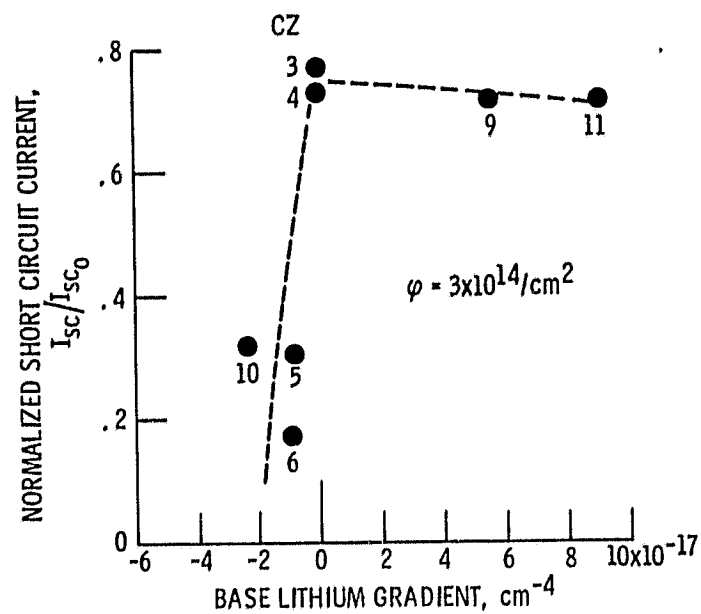


Figure 1. - Normalized short circuit current versus lithium gradients in base.

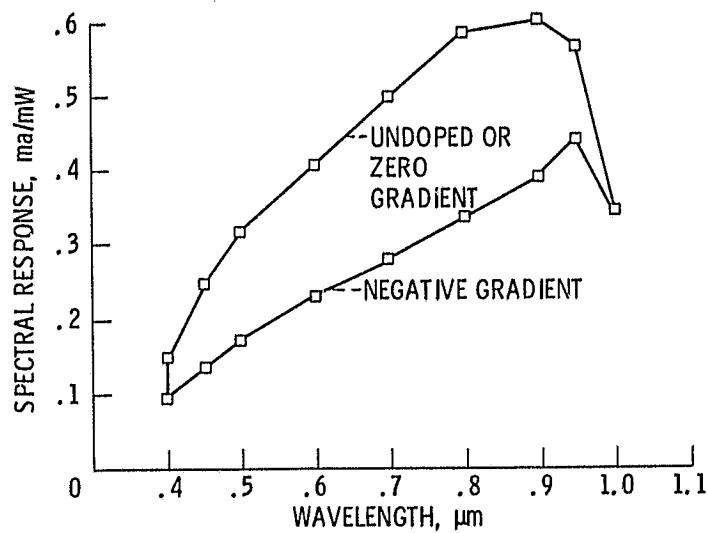


Figure 2. - Spectral response of lithium doped float zone silicon solar cells.

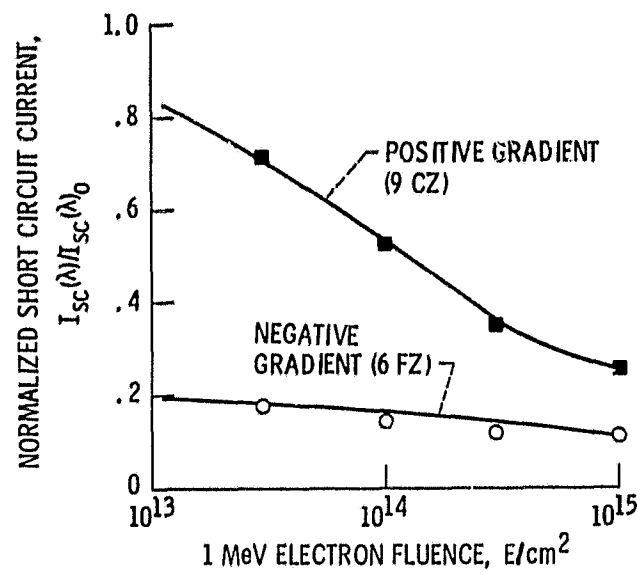


Figure 3. - Normalized short circuit current at 0.95 μm .

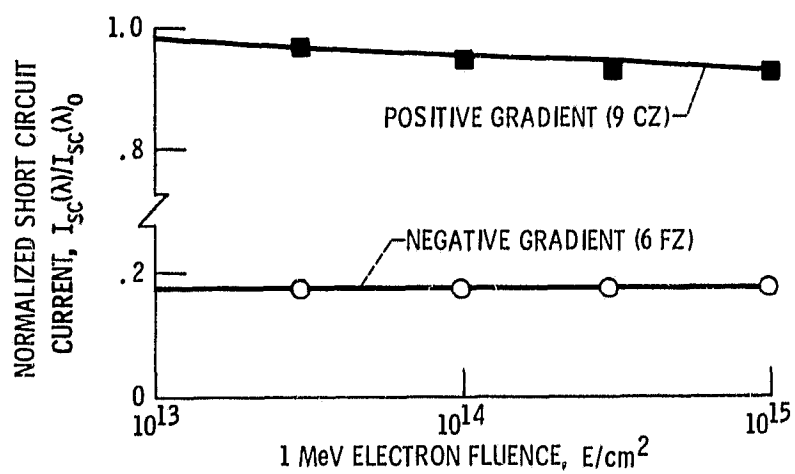


Figure 4. - Normalized short circuit current at 0.45 μm .

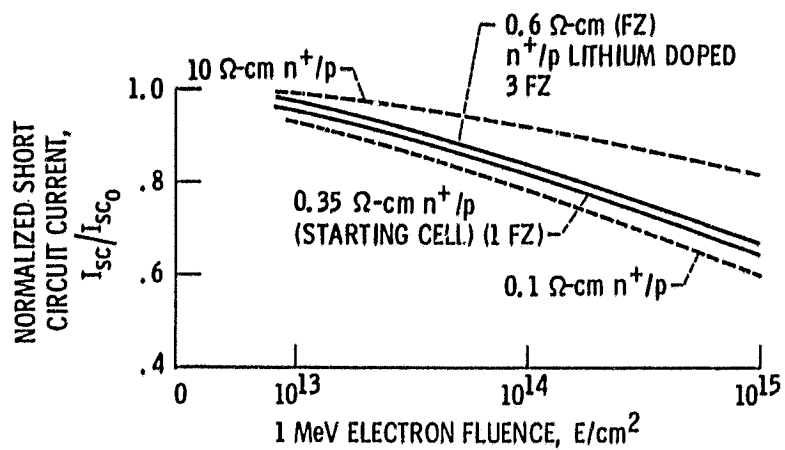


Figure 5. - Variation of normalized short circuit current with electron fluence for FZ cell compared to starting cells and other n^+/p cells.

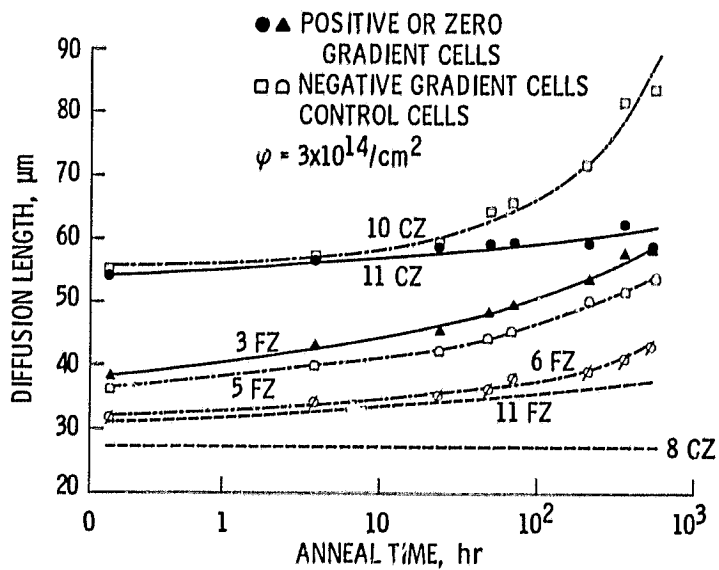


Figure 6. - Diffusion length recovery during room temperature anneal.

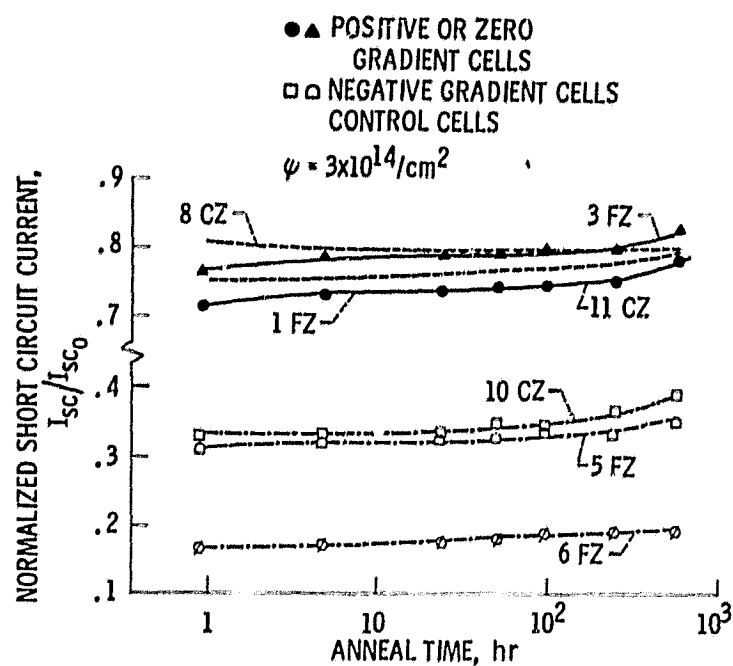


Figure 7. - Normalized short circuit current during room temperature anneal.

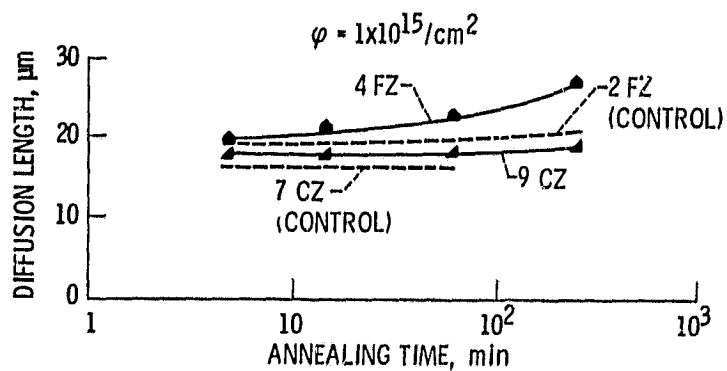


Figure 8. - Diffusion length recovery after annealing at 600°C .

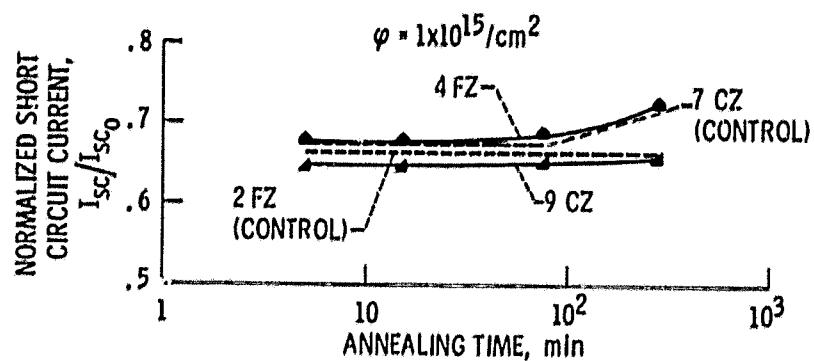


Figure 9. - Short circuit current recovery after annealing at 60° C.

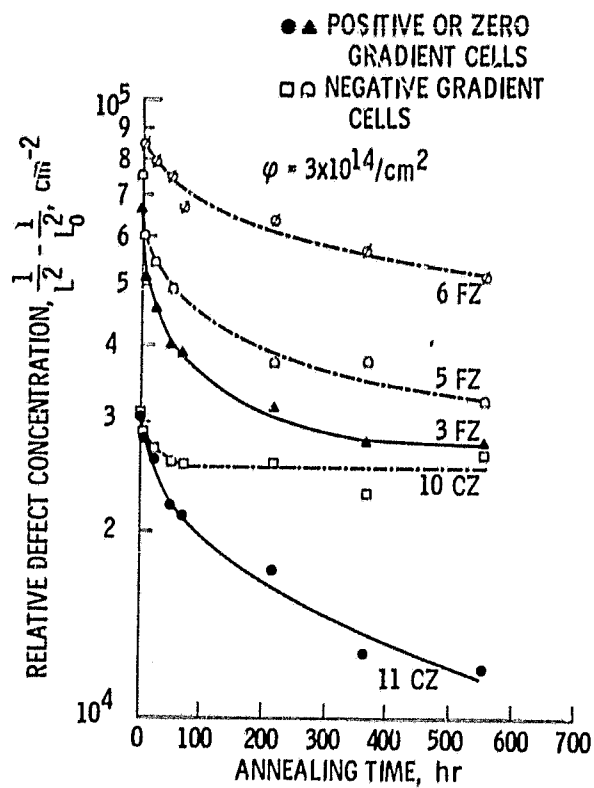


Figure 10. - Annealing kinetics - room temperature.

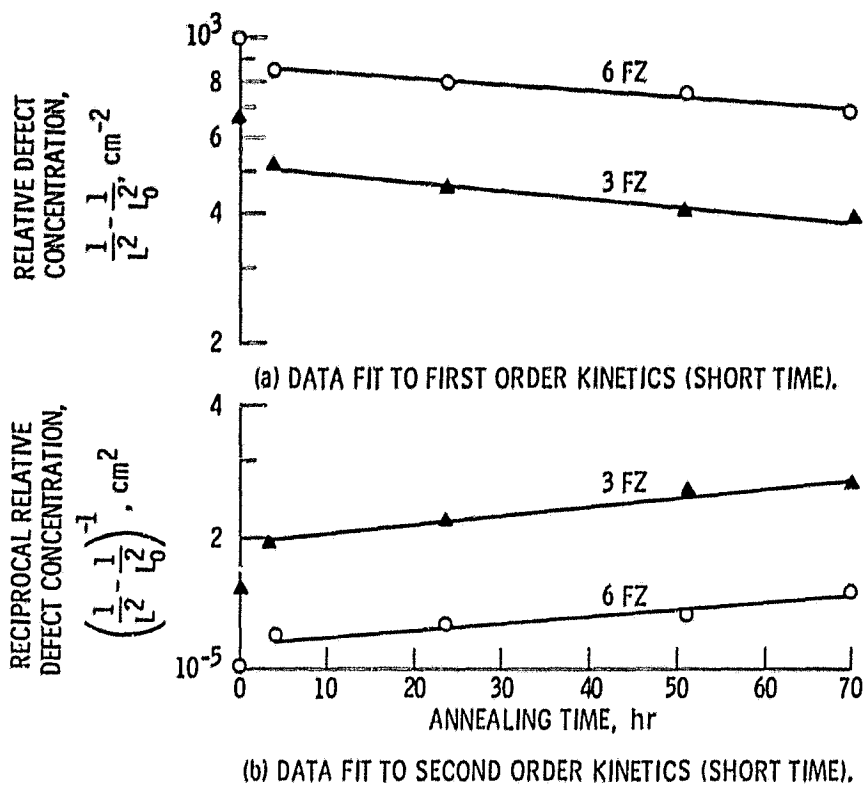


Figure 11 . - Room temperature annealing.

1 Report No. NASA TM-81391		2 Government Accession No.		3 Report's Catalog No.	
4 Title and Subtitle RADIATION DAMAGE IN LITHIUM-COUNTERDOPED N⁺P SILICON SOLAR CELLS				5 Report Date	
7 Author(s) A. M. Hermann, C. K. Swartz, H. W. Brandhorst, Jr., and I. Weinberg				6 Performing Organization Name	
9 Performing Organization Name and Address National Aeronautics and Space Administration Lewis Research Center Cleveland, Ohio 44135				8 Performing Organization Report No. E-301	
12 Sponsoring Agency Name and Address National Aeronautics and Space Administration Washington, D.C. 20546				10 Work Unit No.	
				11 Contract or Grant No.	
				13 Type of Report and Period Covered Technical Memorandum	
				14 Sponsoring Agency Code	
15 Supplementary Notes A. M. Hermann, Tulane University, New Orleans, Louisiana; and C. K. Swartz, H. W. Brandhorst, Jr., and I. Weinberg, NASA Lewis Research Center.					
16 Abstract Lithium-counterdoped n ⁺ /p silicon solar cells were irradiated with 1 MeV electrons and their post-irradiation performance and low temperature annealing properties were compared to that of the 0.35 ohm-cm control cells. Cells fabricated from float zone and Czochralski grown silicon were investigated. It was found that the float zone cells exhibited superior radiation resistance compared to the control cells, while no improvement was noted for the Czochralski grown cells. Room temperature and 60° C annealing studies were conducted. The annealing was found to be a combination of first- and second-order kinetics for short times. The defect migration energy found from the kinetic studies suggests that the principal annealing mechanism is migration of lithium to a radiation induced defect with subsequent neutralization of the defect by combination with lithium. The effects of base lithium gradient were investigated. It was found that cells with negative base lithium gradients exhibited poor radiation resistance and performance compared to those with positive or no lithium gradients, the latter being preferred for overall performance and radiation resistance.					
17. Key Words (Suggested by Author(s)) Solar cells Radiation damage Lithium counter doped Temperature annealing			18. Distribution Statement Unclassified - unlimited STAR Category 44		
19. Security Classif. (of this report) Unclassified		20. Security Classif. (of this page) Unclassified		21. No. of Pages	
				22. Price*	

* For sale by the National Technical Information Service, Springfield, Virginia 22161